J. DRUG DEL. SCI. TECH., 24 (5) 445-451 2014

Visible quantum-dot-based targeted siRNA delivery for HIF-1α gene silencing

HongYan Zhu, JingPing Zhu, AiMei Xie, Yong Lin, BeiBei Zhang, YiFei Wang, Wei Zhang*

Department of Pharmacology, Medical College, Nantong University, No. 19 Qixiu Road, Nantong 226001, China
*Correspondence: zhangwntu@163.com

In the present paper, we synthesized cadmium (Cd) telluride (Te) quantum dots (CdTe QDs) by a hydrothermal method using three different ligands as stabilizers: N-acetyl-L-cysteine (NAC), cysteamine hydrochloride (CA), or 2-(dimethylamino) ethanethiol hydrochloride (DMAE). The results demonstrated that CA-coated CdTe QDs had a higher zeta potential (positive) compared with the NAC- and DMAE-coated CdTe QDs. Furthermore, CA-coated CdTe QDs had greater ability to bind siRNA and greater uptake by human gastric cancer cells (SGC-7901). The release of siRNA from the surface of CdTe QDs was induced by high concentrations of reduced glutathione (GSH). mRNA and protein levels of HIF-1α in SGC-7901 cells were significantly reduced after being treated with the complex of CA-coated CdTe QDs and HIF-1α siRNA under strictly anerobic conditions. In addition, CA-coated CdTe QDs displayed excellent optical properties, good morphology, and low toxicity to normal cells.

Key words: Quantum dots – siRNA – Tumor – Glutathione – HIF-1α.

RNA interference (RNAi) is an emerging technology for sequence-specific gene silencing. RNAi technology has several potentially interesting uses that range from functional detection of genes to targeted gene therapy [1, 2]. However, *in vivo* applications of RNAi technology remain limited due to the lack of an effective delivery system. Major issues associated with its *in vivo* application include poor cellular uptake, minimal endosomal escape, complex dissociation from its carrier. To resolve some of these issues, a number of small interfering RNA (siRNA) delivery systems have been developed. These include liposomes [3,4], lipid nanoparticles [5], macromolecule polymers [6-8], chitosan [9], small peptides [10], viruses [11], and dendriworms [12]. Through improvements in transfection efficiency of siRNA, the aforementioned delivery systems can lead to effective gene silencing. Due to the lack of intrinsic fluorescence capability, the siRNA delivery processes of these systems cannot be visualized directly. It has been shown that luminous quantum dots (QDs) can be used as fluorescence probes for biological imaging [13-16]. As fluorescent biological molecular sensors, QDs have several advantageous properties such as a narrow emission spectrum, broad excitation range, and robustness against photobleaching. QDs are of particular interest in RNAi experiments and could facilitate the visualization of the siRNA delivery process.

Hypoxia-inducible factor 1 (HIF-1) is a type of an oxygen-sensitive transcriptional activator, which is specifically activated in hypoxia [17]. HIF-1 has an effect on metabolism [18], proliferation [19], hematopoiesis [20], angiogenesis [21, 22], and vasotone regulation [23]. HIF-1 is a dimer composed of 2 subtypes: HIF-1α and HIF-1β. In normoxic conditions, HIF-1β is constitutively expressed, whereas HIF-1α is maintained at low steady-state levels. This is due to the degradation of HIF-1α by the proteasome pathway under normoxic conditions [24, 25]. On the contrary, the degradation of proteasome is inhibited under hypoxic conditions, which leads to an increase of HIF-1α under such conditions. The down regulation of HIF-1α during hypoxia has been shown to be associated with the inhibition of tumor vessel development and tumor proliferation [19].

In the present paper, we evaluated the water soluble cadmium (Cd) tellurium (Te) QDs (CdTe QDs) stabilized with ligands with differing surface charge: N-acetyl-L-cysteine (NAC), cysteamine hydrochloride (CA), or 2-(dimethylamino) ethanethiol hydrochloride (DMAE). CdTe QDs were conjugated with HIF-1α siRNA to form QDs-siRNA complexes by simple electrostatic interaction. It is hypothesized that the QDs-siRNA complexes could lead to significant improvements in intracellular delivery of HIF-1α siRNA, and that the release of HIF-1α siRNA would be triggered by high concentrations of glutathione (GSH) in cancer cells. The potential for QDs-siRNA complexes to inhibit HIF-1α mRNA and protein expression will also be investigated. Additionally, we expect QDs to deliver siRNA much more effectively, significantly increase gene silencing, and to be used to visualize the entire siRNA delivery process.

I. MATERIALS AND METHODS

1. Materials

Tellurium (Te) powder, sodium borohydride ($NaBH_4$), cadmium chloride ($CdCl_2 \cdot 2.5H_2O$), NAC, CA, GSH and DMAE were all purchased from Aladdin Reagents (Shanghai, China). 3-(4, 5-dimethylthialzol-2-yl)-2, 5-diphenyltetrazolium bromide (MTT), RPMI 1640, fetal bovine serum (FBS), penicillin, streptomycin, and trypsin were purchased from Gibco Inc. (Shanghai, China). Reagents used for reverse transcriptase-polymerase chain reaction (RT-PCR) and Western blot experiments were acquired from Fermentas China Co., Ltd. (Shenzheng, China). All other chemical agents were all purchased as analytical reagent grade from Shanghai Chemical Reagent Company (Shanghai, China).

2. Synthesis of water-soluble CdTe quantum dots (CdTe QDs)

CdTe QDs were synthesized using the hydrothermal method according to the published methods. Briefly, $NaBH_4$ and Te powder were reacted at a molar ratio of 3:1 in ethanol and deionized water under an N_2 atmosphere. Following the addition of sulphuric acid, H2Te gas was produced, and collected by NaOH solution to prepare the precursor of sodium hydrogen telluride (NaHTe). In addition, $CdCl_2$ and either NAC, CA, DMAE were added under vigorous stirring in an N_2 atmosphere and appropriate pH environment. Fresh NaHTe solution was subsequently added to the prepared precursor solution. Then the sulfydryl of NAC or CA or DMAE was coordinated with the surface of CdTe QDs. The molar ratio of Cd : Te : NAC or CA or DMAE was set to 1.0 : 0.5 : 4.0. Finally, the solution was reflowed at 100 °C to obtain the NAC or CA or DMAE-capped (NAC/CA/DMAE-capped) CdTe QDs. CdTe QDs were then precipitated with cold isopropanol and isolated by centrifugation to remove excess Cd-NAC/CA/DMAE complexes from solution.

3. Characterization of CdTe QDs

Absorption and fluorescence spectra of the prepared CdTe QDs were scanned by using a 754-PC UV-Vis spectrophotometer (Jing-Hua Technological Instrument Corporation, China) and RF-5301PC fluorescence spectrophotometer (λex = 450 nm) (Shimadzu, Japan). Photoluminescence quantum yield of the obtained CdTe QDs was calculated by comparing their emission peak to that of rhodamine 6G (quantum yield = 95 %, absolute ethanol, λex = 525 nm). An FEI Tecnai G2 20s-TWIN electron microscrope (Philips, Netherlands) was used to observe the morphology of CdTe QDs. The size and zeta potential of NAC/CA/DMAE-capped CdTe QDs in 0.01M phosphate buffered saline (PBS) (137 mmol/L NaCl, 2.7 mmol/L KCl, 4.3 mmol/L Na_2HPO_4, 1.4 mmol/L KH2PO4, pH 7.4) were characterized using a Malvern Zetasizer 3000 system (Malvern Instruments Ltd., United Kingdom).

4. Cytotoxicity assay

MTT assays were performed to evaluate the cytotoxicity of the NAC/CA/DMAE-capped CdTe QDs. Briefly, EaHy926 cells from a human umbilical vein cell line, and SGC-7901 cells from a human gastric cancer cell line, were cultured continuously in RPMI 1640 medium containing 10 % (v/v) FBS, penicillin (100 U/mL), and streptomycin (100 μg/mL) at 37 °C in 5 % CO_2. Cells were then plated in 96-well flat-bottomed microtiter plates (Corning Inc, United States). RPMI 1640 medium (200 μL) containing CdTe QDs of concentrations ranging from 2.5 to 80.0 mmol/L was added to the 96-well plates after cells achieved 70-80 % confluence. After 48 h, cells were incubated with MTT for 3 h and then 100 μL DMSO was added to dissolve the intracellular formazan product. Optical density (OD) was detected by Infinite F200 (Tecan Inc, Switzerland) at 490 nm. Cell viability (%) was defined as equal to $(OD_{treated}/OD_{control}) \times 100$ %, where $OD_{treated}$ was the OD obtained in the presence of QDs and $OD_{control}$ was the absorbance of cells that were not treated with CdTe QDs.

5. Electrophoretic mobility shift assay

Binding and releasing abilities of CdTe QDs and HIF-1α siRNA were examined by electrophoretic mobility shift assay (EMSA). Firstly, QDs and siRNA in RNAase-free-water were mixed for 15 min at room temperature at different QDs:siRNA ratios (1:0, 1:1, 1:5, and 1:10). In the meantime, QDs-siRNA complexes were also preincubated with different concentrations of GSH (0.1, 1 and 3 mmol/L) for use in the release assay. Treated samples were loaded onto 4 % agarose gel plates and samples were run at 100 V for approximately 40 min. Finally, the gel images were taken under UV light using a fluorescent gel imaging and analysis system (Vilber Lourmat, France).

6. Intracellular uptake of CdTe QD-siRNA complexes

EaHy926 and SGC-7901 cells were used to study the intracellular uptake study of CdTe QDs-siRNA complexes. Three types of complexes, NAC/CA/DMAE-capped CdTe QDs and siRNA, were prepared in serum-free medium and incubated for 20 min at room temperature. Cells were then transfected with the prepared QDs-siRNA complexes and incubated for 30 min. After transfection, the medium was discarded and the cells were washed three times with PBS. Fluorescent images of the intracellular uptake of CdTe QDs-siRNA complexes were obtained by imaging transferred cells using the fluorescence microscopy (Olympus BX60, Japan), and an excitation wavelength of 488 nm.

7. *In vitro* transfection experiments

SGC-7901 cells were cultured overnight in 6-well plates (Corning Inc., United States) at a density of 1×10^4 per well in order to achieve 60-80 % confluence. For siRNA transfection, cultured cells were washed with PBS and preincubated for 2 h with RPMI 1640 medium without serum and antibiotics. To created QDs-siRNA complexes, siRNA against HIF-1α and CdTe QDs were incubated in RPMI 1640 medium without serum for 20 min at room temperature. Non-specific siRNA (NS siRNA) was used as negative control and also mixed with CdTe QDs for RNA interference (RNAi) experiment. Then pure siRNA (50 nmol/L) and QD-siRNA complexes (50 nmol/L siRNA) were added to each well, respectively, and incubated with SGC-7901 cells in RPMI 1640 medium without serum at 37 °C for 1 h. Then, the serum-free medium was replaced with RPMI 1640 medium with 10 % FBS and cells were incubated for a further 16 h in either normoxic (5 % CO_2, 95 % air) or hypoxic (2 % O_2, 5 % CO_2, 93 % N_2) conditions. Finally, the total RNA and protein was extracted from the transfected cells for further RT-PCR and Western blot experiments.

8. RT-PCR experiment

The total RNA of the transfected SGC-7901 cells was extracted with Trizol. cDNA was synthesized from RNA with the use of RevertAid First Strand cDNA Synthesis Kit. PCR was performed with Bio-rad S1000 (Bio-rad Inc, United States) as follows: 1 cycle, 95 °C, 10 min; 30 cycles, 95 °C, 45 s; 60 °C, 45 s; 72 °C, 60 s; 1 cycle, 72 °C, 5 min. The forward and reverse primers were 5'-CTGCACTCAATCAAGAAGTTGC-3' and 5'-AGTGGTGGCATTAGCAGTAGGT-3', respectively, for HIF-1α mRNA amplification, and 5'-AGCGAGCATCCCCCAAAGTT-3' and 5'-GGGCACGAAGGCTCATCATT-3', respectively, for β-actin amplification. The PCR products were analyzed by 1 % agarose gel electrophoresis (100 V, 30 min).

9. Western blot experiments

Proteins were extracted by lyses buffer (50 mmol/L Tris-HCl, 1 mmol/L EDTA, 100 mmol/L NaCl, 20 mmol/L NaF, 3 mmol/L Na3VO4, 1 mmol/L PMSF, with 1 % Nonidet P-40, and protease inhibitor cocktail) from the transfected SGC-7901cells, separated on a 10 % SDS-PAGE gel by electrophoresis, and transferred to nitrocellulose membranes. The membranes were then washed with TBS (10 mmol/L Tris, 150 mmol/L NaCl) supplemented with 0.05 % (v/v) Tween 20 (TBST) and blocked for 80 min with TBST containing 5 % (w/v) nonfat dried milk. Membranes were probed overnight at 4 °C with antibodies specific for HIF-1a (1:1000) and the primary antibody for GAPDH (1:7000). Membranes were then incubated with IRDye 680-labeled secondary antibodies for 2 h at room temperature and away from sunlight. After washing the membranes three times with TBST at room temperature, immunoreactivity signals were detected with the Odyssey CLx Western Blot detection system (LI-COR Biosciences, United States).

10. Statistical analysis

To find out the difference between two independent samples, t-test was performed by using SPSS (Version 11.5, SPSS Inc., United States). A P value of 0.05 or less was considered significant.

II. RESULTS AND DISCUSSION

1. Synthesis and characterization of CdTe QDs

The NAC/CA/DMAE-capped CdTe quantum dots were synthesized using the procedures for water-soluble CdTe QDs. *Figures 1 and 2* display the absorption and photoluminescence (PL) emission spectra of CdTe QDs prepared at different reaction times. With longer reaction times, both the absorption and photoluminescence emission peaks of nanoparticles exhibited a gradual red shift. As such, the emission peaks of NAC/CA/DMAE-capped CdTe QDs were easily tunable from 517 to 561 nm, 530 to 564 nm, and 500 to 525 nm, respectively, by controlling the reaction times. Because the size distributions of QDs increase with the continuous extension of reaction time and the emission peaks are decided by the sizes of QDs. Quantum yields (QY) of the NAC/CA/DMAE-capped CdTe QDs reached approximately 85, 50 and 9 %, respectively.

The optical qualities of QDs, such as the intensity and stability of fluorescence, depend on pH, reactants molar ratio of the original

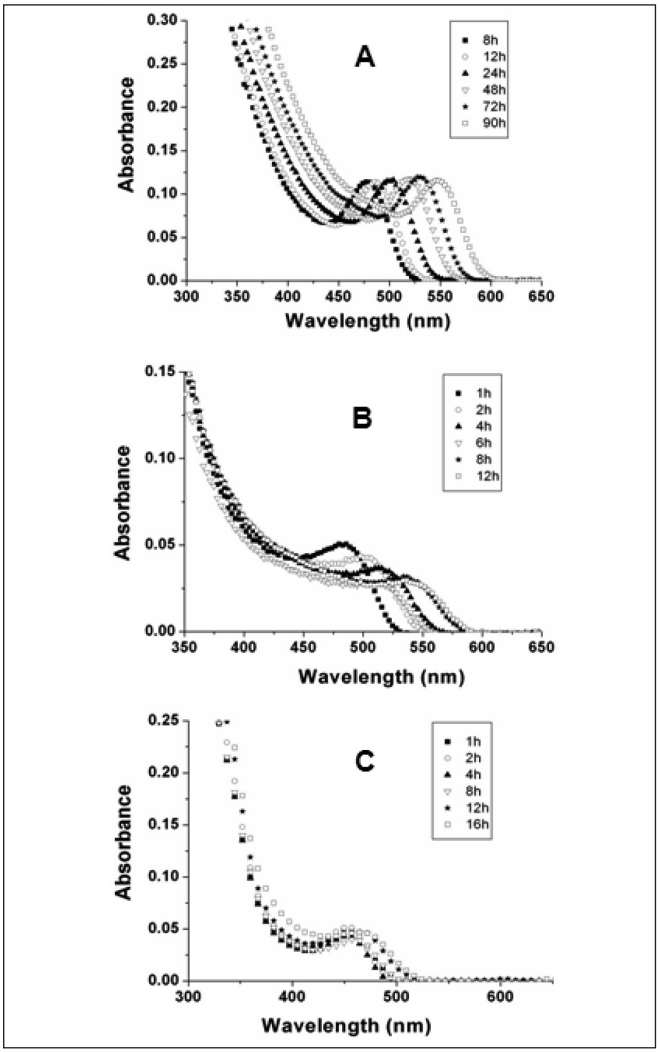

Figure 1 - The absorption spectra of CdTe quantum dots obtained by controlling the reaction time (A: NAC-capped CdTe QDs, B: CA-capped CdTe QDs, C: DMAE-capped CdTe QDs).

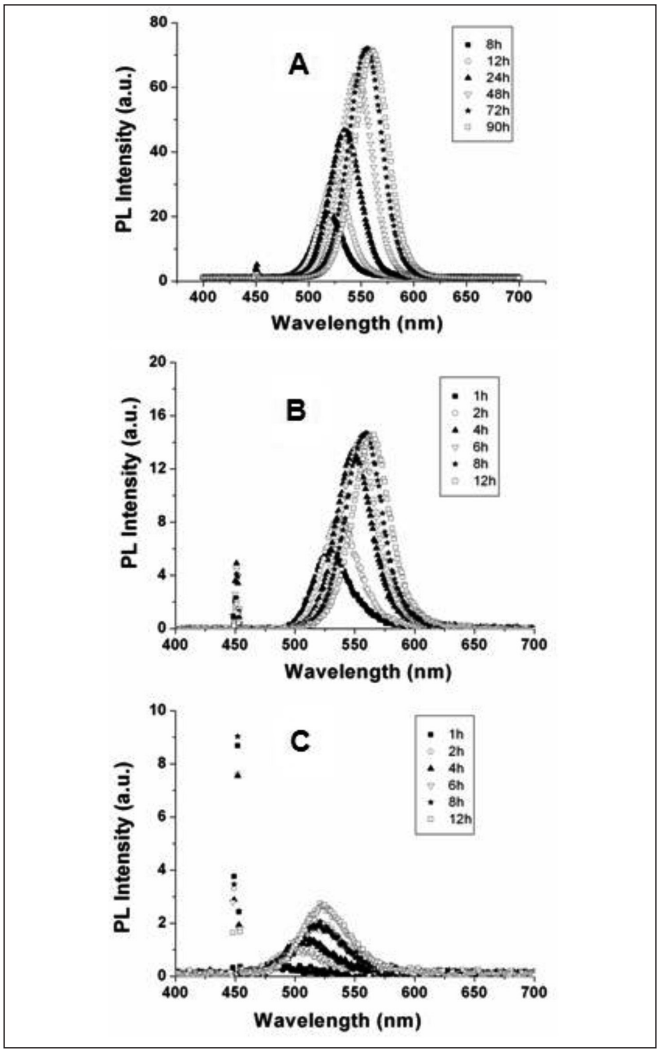

Figure 2 - The PL spectra of CdTe quantum dots obtained by controlling the reaction time (A: NAC-capped CdTe QDs, B: CA-capped CdTe QDs, C: DMAE-capped CdTe QDs).

solution and reaction time. In the present study, the pH of the original solution was optimized for the synthesis of each type of CdTe QDs: pH of 8.5-9.5 was used for NAC-capped CdTe QDs, pH of 6.5-7.5 for CA-capped CdTe QDs, and pH of 7.0-8.0 for DMAE-capped CdTe QDs. Upon synthesis completion, stable QD solutions with a pH between 7.0 and 8.0 were achieved, making fluorescent QDs suitable for use in biological studies.

The morphology of CdTe QDs was investigated using transmission electron microscopy (TEM; λem = 525 nm). *Figure 3* shows a low-magnification TEM image of the prepared QDs. NAC-capped CdTe QDs were almost spherical in shape and had with excellent polydispersity. CA-capped CdTe QDs had a near-spherical profile and exhibited a small degree of aggregation. In contrast, the morphology of DMAE-capped CdTe QDs was irregular with a little poor polydispersity. The average sizes of the NAC-, CA-, and DMAE-capped CdTe QDs were about 2.5, 4 and 5 nm, respectively. The surface charges of CdTe QDs, as measured by zeta potential analysis, were recorded as -13.7, +38.6 and +17.0 mV, respectively, for the NCA-, CA-, and DMAE-capped CdTe QDs.

2.cCytotoxicity of CdTe QDs

An MTT assay was used to evaluate the cytotoxicity of QDs prepared in our lab against EaHy926 and SGC-7901cells. As shown in *Figure 4*, NAC-capped CdTe QDs presented less toxicity at most test doses, compared with CA- and DMAE-capped CdTe QDs. Viabilities

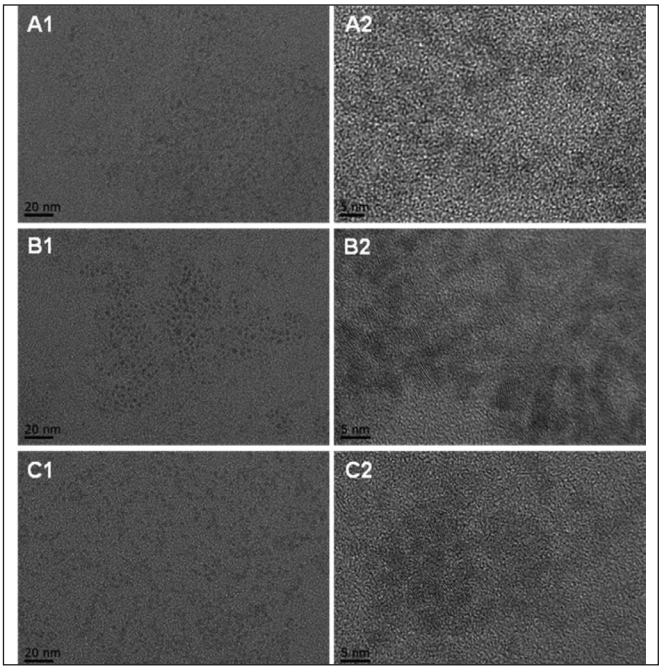

Figure 3 - TEM image of CdTe quantum dots (A: NAC-capped CdTe QDs, B: CA-capped CdTe QDs, C: DMAE-capped CdTe QDs).

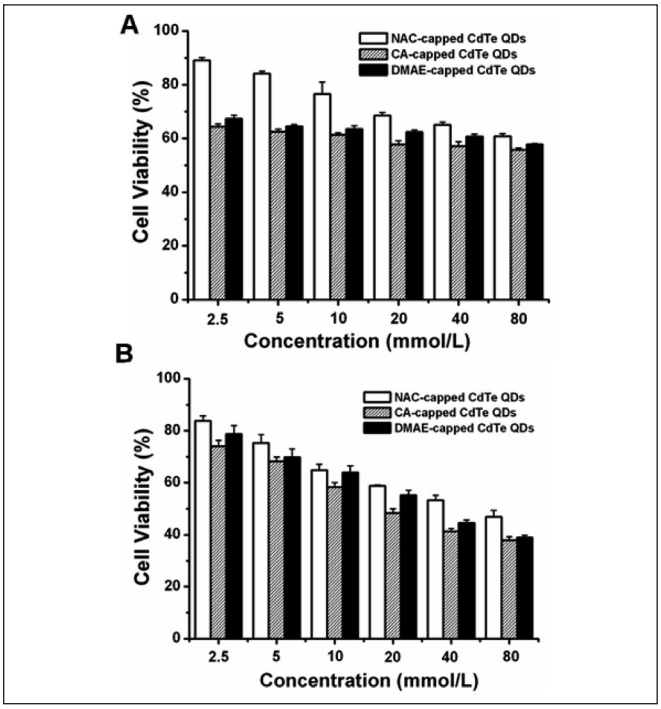

Figure 4 - *In vitro* cytotoxicity of QDs determined by MTT assay: (A) human umbilical vein cells (EaHy926 cells) cultured with CdTe QDs; (B) human gastric cancer cells (SGC-7901 cells) cultured with CdTe QDs (n = 3).

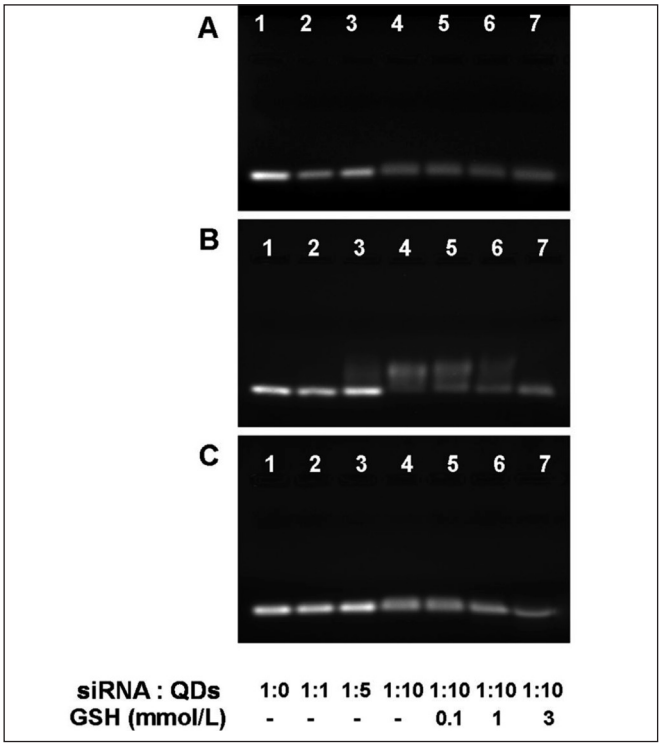

Figure 5 - The agarose gel electrophoresis of CdTe QDs and siRNA mixture with different ratios (siRNA:QDs in lanes 1-4 was 1:0, 1:1, 1:5 and 1:10, respectively); the mixture of siRNA and QDs at stoichiometry (1:10) incubated with different concentrations of GSH (lanes 5-7: 0.1, 1 and 3mmol/L) (A: NAC-capped CdTe QDs, B: CA-capped CdTe QDs, C: DMAE-capped CdTe QDs).

of EaHy926 and SGC-7901cells were maintained at 61 % and 47 %, respectively, in the presence of NAC-capped CdTe QDs at the highest concentration (80 mmol/L). At the lowest concentration (2.5 mmol/L), which incidentally was significantly higher than the concentration used in the cell imaging and RNAi experiments, average EaHy926 and SGC-7901 cells viability was recorded as 89 and 83 %, respectively. In contrast, CA- and DMAE-capped CdTe QDs were associated with greater cytotoxicity. Viability of EaHy926 cells was 56 and 58 % in the presence of 80 mmol/L CA- and DMAE-capped CdTe QDs, respectively. Viability of SGC-7901 cells was approximately 38 and 39 % in the presence of 80 mmol/L CA- and DMAE-capped CdTe QDs, respectively. Lower concentrations of CA- and DMAE-capped CdTe QDs were less cytotoxic.

The cytotoxicity of CdTe QDs might be related to the factors such as the choice of stabilizer, its structure, and zeta potential. To the best of our knowledge, there are two important reasons for QDs causing cytotoxicity: i) a bio-toxic ligand coating the QDs; ii) the heavy metals of QDs inducing oxidative stress in cells. NAC, the ligand we chose to synthesize QDs, is an innocuous, stable, environmentally friendly and biocompatible ligand which could reduce the toxicity of QDs compared with CA- and DMAE-capped CdTe QDs. NAC can also form a stable complex with Cd^{2+} and improve stability of QDs [26, 27]. Such a NAC-capped structure could reduce the surface defects of QDs and also inhibit the release of Cd^{2+} from QDs, which can notably lessen the toxicity of QDs. Meanwhile, NAC has previously been found to protect cells against oxidative stress [28]. Therefore, using NAC to stabilize QDs might protect cells against QDs-induced cytotoxicity. The cytotoxicity of QDs may also depend on their zeta potential. From the zeta potential results of CdTe QDs in this study, it is known that NAC-capped CdTe QDs have a negative surface charge, but CA- and DMAE-capped CdTe QDs both have a positive surface charge. It is well known that the transmembrane potential of mammalian cells is usually negative. Indeed, the transmembrane potential of tumor cells is more negative than that of normal cells [29]. The positively charged CA- and DMAE-capped CdTe QDs have the potential to enter the cytoplasm of tumor cell membranes due to electrostatic attraction, whereas with negatively charged NAC-capped CdTe QDs would be electrostatically repulsed. Therefore, NAC-capped CdTe QDs would most likely cause less toxicity than CA- and DMAE-capped CdTe QDs. In addition, the toxicity of CA/DMAE-capped CdTe QDs to cancer cells was much higher than that to healthy cells, which could be explained by the electrostatic difference between normal and tumor cells. The transmembrane potential of tumor cells is more negative than normal cells. So positively charged CdTe QDs could combine and enter cancer cells rather than normal cells, which led to more toxicity to tumor cells. Experiments of investigating *in vitro* cellular uptake had been done to confirm this hypothesis.

3. Binding and releasing ability of siRNA and CdTe QDs

EMSA was used to confirm the binding and releasing ability of siRNA and CdTe QDs. As shown in Figure 5, the QDs and siRNA complex was inhibited from moving towards the positive electrode in agarose gel, especially when the mole ratio of QDs/siRNA was just 1:10 (at lane 4). Meanwhile, almost same amounts of siRNA molecules were detected at the same site of pure siRNA (lane 1) when the QDs were not enough (at lane 2 and 3, QDs:siRNA was 1:1 and 1:5 respectively). Under the appropriate proportion of siRNA and QDs, the negative charges of siRNA could be counteracted by the positively charged QDs. So the movement of siRNA towards the positive electrode would be slowed down (Figure 5 B), which further confirmed that positive zeta potential values were equal to conjugate negative siRNA. The results of the releasing experiment indicated that the mobility of siRNA recovered completely when the final concentration of GSH reached 3 mmol/L (lane 7), while there was no detectable siRNA release when the QDs-siRNA complexes were pretreated with 0.1 mmol/L GSH (lane 5). These results suggested that the release of siRNA could be induced in the presence of high concentrations of GSH.

Presently, there are three main challenges in drug delivery systems, including drug encapsulation, cellular internalization, and cellular release [30]. Several methods, including hydrolysis under low pH [31], enzymatic degradation [32] and certain chemical reactions [33], have been developed to overcome challenges with cellular release. Recently, GSH-triggered release systems have attracted growing attention due to the specificity of GSH in living system. The first advantage is that GSH/ glutathione disulfide (GSSG) ratio could change according to the redox in the environment of cells [34]. Secondly, the concentration of GSH in erythrocytes (2 mmol/L) [35] and in liver cells (10 mmol/L) [36] is significantly higher than that in the extracellular environment (2 μmol/L in red plasma [37]). This distinct concentration difference of GSH inside and outside cells provides a potential for GSH-dependent selective intracellular release, which has been confirmed by EMSA.

4. *In vitro* cellular uptake of CdTe QD-siRNA complexes

The findings of the fluorescent microscopy analysis of cellular uptake of CdTe QD-siRNA complexes in normal (EaHy926) and tumor (SGC-7901) cells are shown in *Figure 6*. CA- and DMAE-capped CdTe QDs-siRNA complexes attached to the tumor cell membrane immediately after being added into the culture medium. Following internalization, which occurred within 30 min, these complexes accumulated at a region outside the cell nucleus. Therefore, CA- and DMAE-capped CdTe QDs-siRNA complexes emitted green fluorescence in the tumor cells (*Figure 6*, panels b2 and c2), while the negative NAC-capped CdTe QDs did not. The results demonstrated that positively charged CA/DMAE-capped CdTe QDs increased the transfection ability of siRNA. In addition, the CA/DMAE-capped CdTe QDs-siRNA complexes underwent active and directional motions in tumor cells but not in normal cells. That finding can be explained by the fact that the transmembrane potential of tumor cells is more negative than normal cells, which lead to positively charged CdTe QDs combining with cancer cells rather than normal cells. In summary, CA/DMAE-capped QD-siRNA complexes may provide promising targets for tumor cells.

5. Gene silencing efficiency of CdTe QD-siRNA complexes

The gene silencing efficiency of QDs was investigated by RT-PCR and Western-blot experiments, using pure siRNA as contrast. The siRNA was devised for HIF-1α mRNA and based on the same siRNA concentration and the optimized amount for each transfection reagent. siRNA-QDs complexes were prepared by mixing the QDs with siRNA to achieve complexes. The optimized siRNA:QDs molar ratio was 1:10 which was determined to be the optimal ratio based on the findings of the EMSA experiment. The performance results showed that the expression levels of HIF-1α mRNA in SGC-7901 cells under hypoxic conditions were significantly higher than that in cells in normoxic conditions ($P<0.01$) (*Figure 7*). Additionally, the expression levels of HIF-1α mRNA in SGC-7901cells under hypoxic conditions were reduced after being treated with either CA- or DMAE-capped CdTe QDs-siRNA complexes ($P < 0.01$) (*Figure 7*). By using CA-capped QDs-siRNA complexes, we were able to achieve excellent gene silencing efficiency against HIF-1α mRNA.

We also investigated whether treatment with CdTe QDs-siRNA complexes led to altered expression of the HIF-1α protein in SGC-7901 cells was also investigated. As shown in *Figure 8*, SGC-7901 cells in hypoxic conditions expressed higher levels of HIF-1α protein than cells in normoxic conditions ($P < 0.05$). Strong down-regulation of HIF-1α at the protein level in GC-7901 cells was found after treatment with CA- and DMAE-capped CdTe QDs-siRNA complexes ($P < 0.01$). However, expressions of HIF-1α protein were not significantly affected by treatment with pure siRNA or NAC-capped QD-siRNA complexes treatment ($P > 0.05$). This may be explained by the fact

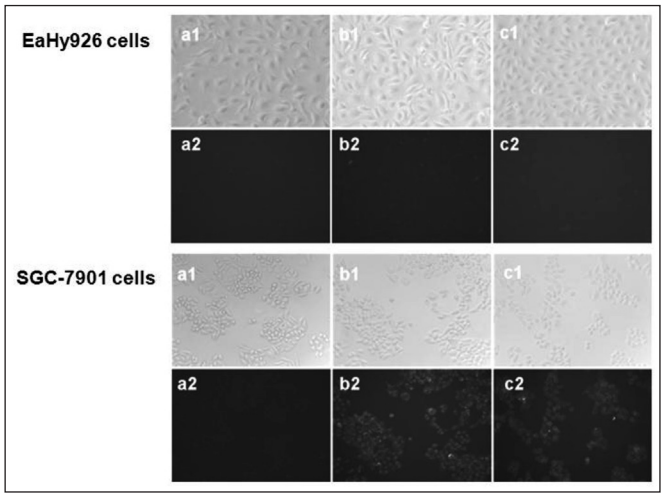

Figure 6 - The intracellular uptake of CdTe QDs in EaHy926 cells and SGC-7901 cells using inverted fluorescence microscope: 1: bright-field and 2: fluorescence images of EaHy926 cells and SGC-7901 cells treated with CdTe QDs (a: NAC-capped CdTe QDs, b: CA-capped CdTe QDs, c: DMAE-capped CdTe QDs).

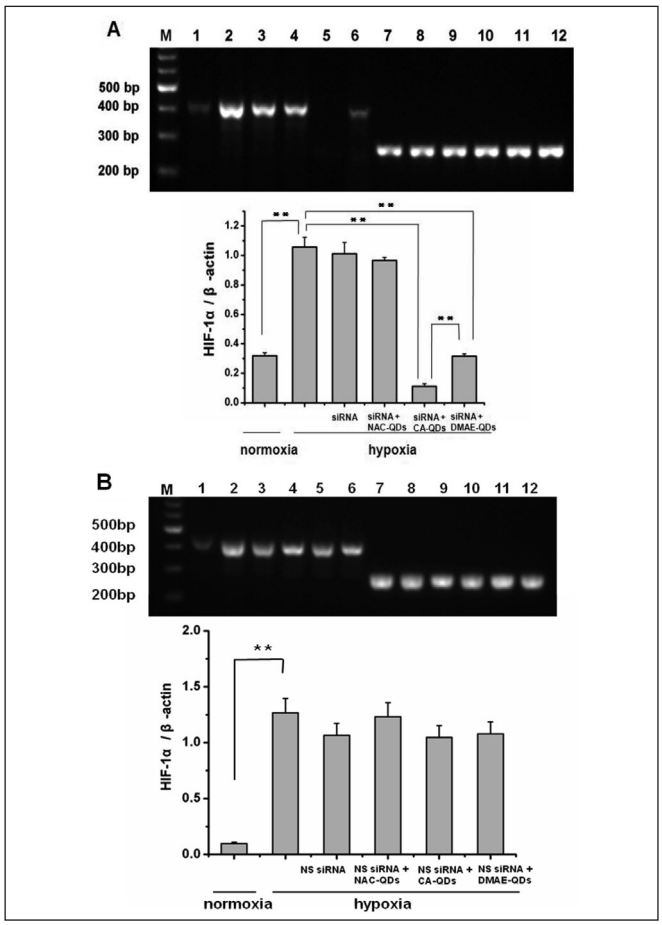

Figure 7 - RT-PCR results of QD-siRNA complexes with electrophoresis mobility-shift assays in 1 % agarose gel to determine HIF-1α mRNA levels in SGC-7901 cells after transfection (M: marker, 1-6: HIF-1α mRNA levels, 7-12: β-actin mRNA levels (1, 7: control in normoxia; 2, 8: control in hypoxia; 3, 9: pure siRNA (A: HIF-1α siRNA, B: NS siRNA) in hypoxia; 4, 10: NAC-capped QD and siRNA (A: HIF-1α siRNA, B: NS siRNA) complexes in hypoxia; 5, 11: CA-capped QD and siRNA (A: HIF-1α siRNA, B: NS siRNA) complexes in hypoxia; 6, 12: DMAE-capped QD and siRNA (A: HIF-1α siRNA, B: NS siRNA) complexes in hypoxia)) ($n = 3$) (**$P < 0.01$, *$P < 0.05$).

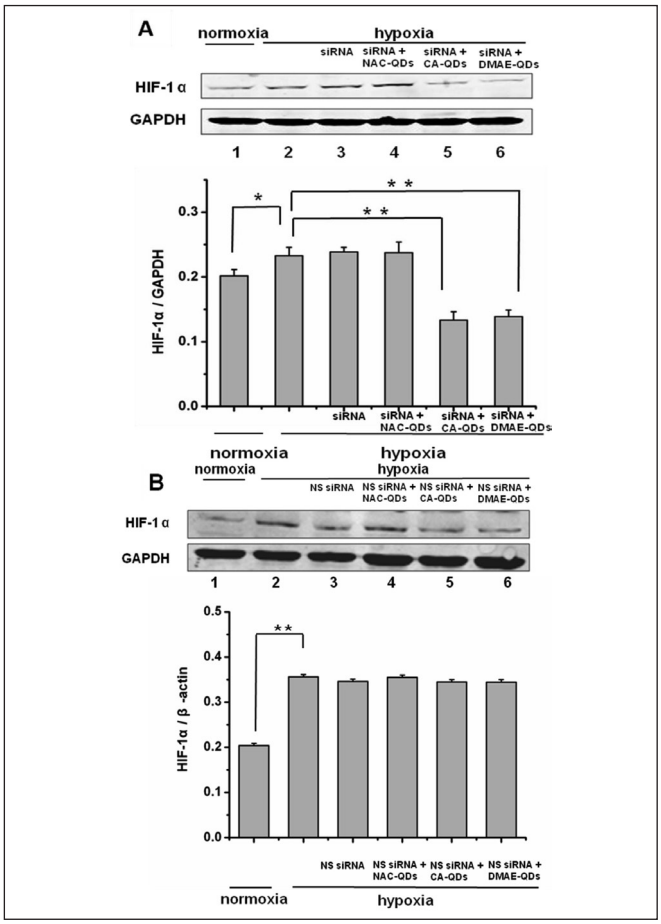

Figure 8 - HIF-1α protein levels in SGC-7901 cells under normoxic or hypoxic conditions by Western Blot (lane 1: HIF-1α protein levels under normoxia without treatment; lane 2: HIF-1α protein levels under hypoxia without treatment; lane 3: HIF-1α protein levels under hypoxia after being treated with pure siRNA (A: HIF-1α siRNA, B: NS siRNA); lane 4: HIF-1α protein levels under hypoxia after being treated with NAC-capped QD and siRNA (A: HIF-1α siRNA, B: NS siRNA) complexes; lane 5: HIF-1α protein levels under hypoxia after being treated with CA-capped QD and siRNA (A: HIF-1α siRNA, B: NS siRNA) complexes; lane 6: HIF-1α protein levels under hypoxia after being treated with DMAE-capped QD and siRNA (A: HIF-1α siRNA, B: NS siRNA) complexes) (n=3) (**P<0.01).

that NAC-capped CdTe QDs complexes have a negative zeta potential, which leads to low combined capacity with siRNA and weaker transfection efficiency in tumor cells. This requires further validation with electrophoretic mobility shift assay and intracellular uptake experiments of CdTe QD-siRNA complexes could prove it.

To further investigate the RNAi potential of CdTe QD-siRNA complexes, the NS siRNA was used as negative control. The results of RT-PCR and Western-blot show that the pure NS siRNA and NAC/CA/DMAE-capped QD-NS siRNA complexes couldn't suppress the expression of HIF-1α mRNA and protein obviously, which further confirmed gene silencing efficiency of the complexes of CdTe QD and siRNA against HIF-1α.

*

Water-soluble CdTe QDs coated with NAC and CA exhibited optimal optical properties and good morphology, high-resolution and low toxicity to normal cells. These properties make them an ideal inorganic material for biomaterial applications. Furthermore, compared with the NAC- and DMAE-coated CdTe QDs, the CA coated CdTe QDs had a more positive zeta potential, increased ability to bind and release siRNA that was induced by reduced GSH, and greater uptake by the human gastric cancer cells (SGC-7901). The mRNA and protein levels of HIF-1α in SGC-7901 cells were significantly reduced after being treated with the complexes of CA-capped CdTe QDs and HIF-1α siRNA under strictly anaerobic conditions. These results suggest that CA-modified CdTe QDs could be used as excellent siRNA carriers to effectively silence a target gene, in addition to being useful as fluorescence probes for analyzing intracellular siRNA delivery processes.

REFERENCES

1. Kim D.H., Rossi J.J. - Strategies for silencing human disease using RNA interference. - Nat. Rev. Genet., **8**, 173-184, 2007.
2. Rana T.M. - Illuminating the silence: understanding the structure and function of small RNAs. - Nat. Rev. Mol. Cell Biol., **8**, 23-36, 2007.
3. Landen C.N., Chavez-Reyes A., Bucana C., Schmandt R., Deavers M.T., Lopez-Berestein G., Sood A.K. - Therapeutic EphA2 gene targeting *in vivo* using neutral liposomal small interfering RNA delivery. - Cancer Res., **65**, 6910-6918, 2005.
4. Zimmermann T.S., Lee A.C., Akinc A., Bramlage B., Bumcrot D., Fedoruk M.N., Harborth J., Heyes J.A., Jeffs L.B., John M., Judge A.D., Lam K., McClintock K., Nechev L.V., Palmer L.R., Racie T., Röhl I., Seiffert S., Shanmugam S., Sood V., Soutschek J., Toudjarska I., Wheat A.J., Yaworski E., Zedalis W., Koteliansky V., Manoharan M., Vornlocher H.P., MacLachlan I. - RNAi-mediated gene silencing in non-human primates. - Nature, **441**, 111-114, 2006.
5. Huang Y.H., Bao Y., Peng W., Goldberg M., Love K., Bumcrot D.A., Cole G., Langer R., Anderson D.G., Sawicki J.A. - Claudin-3 gene silencing with siRNA suppresses ovarian tumor growth and metastasis. - Proc. Natl. Acad. Sci. USA, **106**, 3426-3430, 2009.
6. Park K., Lee M.Y., Kim K.S., Hahn S.K. - Target specific tumor treatment by VEGF siRNA complexed with reducible polyethyleneimine-hyaluronic acid conjugate. - Biomaterials, **31**, 5258-5265, 2010.
7. Manohar M., Pradeep K., Ashwani K.S. - Amphiphilic polyethylenimine polymers mediate efficient delivery of DNA and siRNA in mammalian cells. - Mol. BioSyst., **9**, 780-791, 2013.
8. Aliabadi H.M., Mahdipoor P., Uludağ H. - Polymeric delivery of siRNA for dual silencing of Mcl-1 and P-glycoprotein and apoptosis induction in drug-resistant breast cancer cells. - Cancer Gene Ther., **20**, 169-177, 2013.
9. Andersen M.O., Howard K.A., Paludan S.R., Besenbacher F., Kjems J. - Delivery of siRNA from lyophilized polymeric surfaces. - Biomaterials, **29**, 506-512, 2008.
10. Alexander H. van A., Andrea B., Hesta M., Petra H.M., Bovee-Geurts, Staffan L., Wouter P.R. Verdurmen, Mattias H., Ülo L., Olaf H., Roland B. - Molecular parameters of siRNA-cell penetrating peptide nanocomplexes for efficient cellular delivery. - ACS Nano, **7**, 3797-3807, 2013.
11. Grimm D., Streetz K.L., Jopling C.L., Storm T.A., Pandey K., Davis C.R., Marion P., Salazar F., Kay M.A. - Fatality in mice due to oversaturation of cellular microRNA/short hairpin RNA pathways. - Nature, **441**, 537-541, 2006.
12. Agrawal A., Min D.H., Singh N., Zhu H., Birjiniuk A., von Maltzahn G., Harris T.J., Xing D., Woolfenden S.D., Sharp P.A., Charest A., Bhatia S. - Functional delivery of siRNA in mice using dendriworms. - ACS Nano, **3**, 2495-2504, 2009.
13. Michalet X., Pinaud F.F., Bentolila L.A., Tsay J.M., Doose S., Li J.J., Sundaresan G., Wu A.M., Gambhir S.S., Weiss S. - Quantum dots for live cells, *in vivo* imaging, and diagnostics. - Science, **307**, 538-544, 2005.
14. Han S., Mu Y., Zhu Q., Gao Y., Li Z., Jin Q., Jin W. - Au: CdHgTe quantum dots for *in vivo* tumor-targeted multispectral fluorescence imaging. - Anal. Bioanal. Chem., **403**, 1345-1352, 2012.
15. Li J.J., Zhu J.J. - Quantum dots for fluorescent biosensing and bio-imaging applications. - Analyst, **138**, 2506-2515, 2013.

16. Medintz I.L., Uyeda H.T., Goldman E.R., Mattoussi H. - Quantum dot bioconjugates for imaging, labelling and sensing. - Nat. Mater., **4**, 435-446, 2005.
17. Wang G.L., Semenza G.L. - General involvement of hypoxia-inducible factor 1 in transcriptional response to hypoxia. - Proc. Natl. Acad. Sci. USA, **90**, 4304-4308, 1993.
18. Semenza G.L., Roth P.H., Fang H.M., Wang G.L. - Transcriptional regulation of genes encoding glycolytic enzymes by hypoxia-inducible factor 1. - J. Biol. Chem., **269**, 23757-23763, 1994.
19. Carmeliet P., Dor Y., Herbert J.M., Fukumura D., Brusselmans K., Dewerchin M., Neeman M., Bono F., Abramovitch R., Maxwell P., Koch C.J., Ratcliffe P., Moons L., Jain R.K., Collen D., Keshert E. - Role of HIF-1 alpha in hypoxia-mediated apoptosis, cell proliferation and tumour angiogenesis. - Nature, **30**, 485-490, 1998.
20. Lacombe C., Mayeux P. - Biology of erythropoietin. - Haematologica, **83**, 724-732, 1998.
21. Liu Y., Cox S.R., Morita T., Kourembanas S. - Hypoxia regulates vascular endothelial growth factor gene expression in endothelial cells. Identification of a 5' enhancer. - Circ. Res., **77**, 638-643, 1995.
22. Rose F., Grimminger F., Appel J., Heller M., Pies V., Weissmann N., Fink L., Schmidt S., Krick S., Camenisch G., Gassmann M., Seeger W., Hänze J. - Hypoxic pulmonary artery fibroblasts trigger proliferation of vascular smooth muscle cells: role of hypoxia-inducible transcription factors. - FASEB J., **16**, 1660-1661, 2002.
23. Kourembanas S., Morita T., Christou H., Liu Y., Koike H., Brodsky D., Arthur V., Mitsial S.A. - Hypoxic responses of vascular cells. - Chest, **114**, 25-28, 1998.
24. Jaakkola P., Mole D.R., Tian Y.M., Wilson M.I., Gielbert J., Gaskell S.J., von Kriegsheim A., Hebestreit H.F., Mukherji M., Schofield C.J., Maxwell P.H., Pugh C.W., Ratcliffe P.J. - Targeting of HIF-alpha to the von Hippel-Lindau ubiquitylation complex by O2-regulated prolyl hydroxylation. - Science, **292**, 468-472, 2001.
25. Bruick R., McKnight S.L. - A conserved family of prolyl-4-hydroxylases that modify HIF. - Science, **294**, 1337-1340, 2001.
26. Zhao D., He Z.K., Chan W.H., Choi M.F. Martin. - Synthesis and characterization of high-quality water-soluble near-infrared-emitting CdTe/CdS quantum dots capped by N-acetyl-l-cysteine via hydrothermal method. - J. Phys. Chem. C, **113**, 1293-1300, 2009.
27. Grinberg L., Fibach E., Amer J., Atlas D. - N-acetylcysteine amide, a novel cell-permeating thiol, restores cellular glutathione and protects human red blood cells from oxidative stress. - Free Radical Biol. Med., **38**, 136-145, 2005.
28. Pinho R.A., Silveira P.C., Silva L.A., Luiz Streck E., Dal-Pizzol F., F. Moreira J.C. - N-acetylcysteine and deferoxamine reduce pulmonary oxidative stress and inflammation in rats after coal dust exposure. - Environ Res., **99**, 355-360, 2005.
29. Forrester J.A., Ambrose E.J., Stoker M.G.P. - Microelectrophoresis of normal and transformed clones of hamster kidney fibroblasts. - Nature (Lond.), **201**, 945-946, 1964.
30. Han G., Chari N.S., Verma A., Hong R., Martin C.T., Rotello V.M. - Controlled recovery of the transcription of nanoparticle-bound DNA by intracellular concentratios of glutathione. - Bioconjug Chem., **16**, 1356-1359, 2005.
31. Ulbrich K., Subr V. - Polymeric anticancer drugs with pH-controlled activation. - Adv. Drug Deliv. Rev., **56**, 1023-1050, 2004.
32. Rooseboom M., Commandeur J.N.M., Vermeulen N.P.E. - Enzyme-catalyzed activation of anticancer prodrugs. - Pharmacol Rev., **56**, 53-102, 2004.
33. Kam N.W.S, Liu Z., Dai H. - Functionalization of carbon nanotubes via cleavable disulfide bonds for efficient intracellular delivery of siRNA and potent gene silencing. - J. Am. Chem. Soc., **127**, 12492-12493, 2005.
34. Wang X., Cai X., Hu J., Shao N., Wang F., Zhang Q., Xiao J., Cheng Y. - Glutathione-triggered "off-on" release of anticancer drugs from dendrimer-encapsulated gold nanoparticles. - J. Am. Chem. Soc., **135**, 9805-9810, 2013.
35. Hassan S.S.M., Rechnitz G.A. - Determination of glutathione and glutathione reductase with a silver sulfide membrane electrode. - Anal. Chem., **54**, 1972-1976, 1982.
36. Anderson M.E. - Glutathione: an overview of biosynthesis and modulation. - Chem. Biol. Interact., **112**, 1-14, 1998.
37. Jones D.P., Carlson J.L., Samiec P.S., Sternberg P. Jr, Mody V.C. Jr, Reed R.L., Brown L.A. - Glutathione measurement in human plasma. Evaluation of sample collection, storage and derivatization conditions for analysis of dansyl derivatives by HPLC. - Clin. Chim. Acta., **275**, 175-184, 1998.

ACKNOWLEDGEMENTS

This research was supported by the Natural Science Foundation Committee of China (NSFC 81202467, 81302628), the Natural Science Foundation of Jiangsu Province in China (BK2012232, BK2011389), the Natural Science Research Project of Universities in Jiangsu Province of China (11KJB350004) and a project funded by the Priority Academic Program Development of Jiangsu Higher Education Institutions.

MANUSCRIPT

Received 17 February 2014, accepted for publication 2 July 2014.